Journal of Materials Science: Materials in Electronics (2020) 31:3119–3129
https://doi.org/10.1007/s10854-020-02858-1

Mesoporous Gd_2O_3/NiS_2 microspheres: a novel electrode for energy storage applications

S. Dhanalakshmi[1] · A. Mathi Vathani[2] · V. Muthuraj[1] · N. Prithivikumaran[2] · S. Karuthapandian[1]

Received: 8 September 2019 / Accepted: 3 January 2020 / Published online: 10 January 2020

Abstract
Development of novel Faradic electrode with excellent rate capability and long-lasting characteristics determines the performance of supercapacitor (SC) in current scenario. Rare-earth metal oxides have received considerable attention in SC domain with high volumetric energy density and capacitive performance. In this context, we have fabricated gadolinia/nickel sulphide nanocomposite via simple chemistry approach followed by two step hydrothermal method. Especially, the gadolinia/nickel sulphide nanocomposite synthesized in the current study offers high specific capacitance (354 F g^{-1} at a constant current density of 0.5 A g^{-1}), low charge transfer resistance (6.37 Ω) and outstanding cycle life (1.3% loss capacitance loss even after 5000 continuous charge/discharge cycles). Such enduring energy characteristics of gadolinia based nanocomposite will create a huge impact in the future energy storage systems

1 Introduction

Ever growing energy demands and inadequacy of natural resources pushes us to derive the alternate sustainable energy supply in eco-friendly manner. Since, the electrochemical energy storage systems (supercapacitors, SCs, lithium ion batteries, fuel cells) [1–3] play a significant role in the context of energy demand over the past decades. Of these, SCs are considered as the most deserved candidates in energy storage systems on account of their superior features like fast charge/discharge capabilities, excellent cycle life (10^5–10^6 cycles), wide operating temperature ranges, easy to handle and even low cost also [4–6].

But, the low power density of SCs still remains a big hurdle in energy relay while they are comparable with batteries. So, keen interest has been devoted by the research community to design a novel SC with high volumetric energy density. The setback in SC has been overcome by improving the capacity of the electrode material having excellent electrochemical properties with tunable porous architectures. Such porous architectures allow maximum utilization of electrode materials to greater extent. The stabilized SC that can store/deliver high energy, either by fast Faradic redox phenomenon (pseudocapacitors, more advantageous) or reversible ion adsorption at electrode/electrolyte interfaces (electric double layer capacitor, EDLC) [7, 8].

Graphene, carbon nanotubes (SWCNT, MWCNT), activated carbon and natural derived carbon forms [9, 10] are employed as the prominent candidates in EDLC owing to their layered structure, high specific surface area and excellent conductivity. Poor capacity/energy density of carbonaceous materials hinders their practical applications. Transition metal hydroxides, metal oxides, metal sulphides, conducting polymers are the basic building blocks of Faradic capacitor [11, 12]. Faradic electroactive materials provides high capacity (comparable with theoretical capacity), power density and cycle life due to their awesome qualities such as multiple redox states (+4, +3, +2, +1), high electron affinity and easy to synthesis any desirable architectures.

Despite these fruitful electrodes provide salient features, the research community have a third eye on rare-earth-based elements. Rare-earth-based metal complexes receiving much interest in research domain owing to their positive merits that includes fair electronic configuration, co-ordination chemistry, attracting magnetic properties and energy storage

Electronic supplementary material The online version of this article (https://doi.org/10.1007/s10854-020-02858-1) contains supplementary material, which is available to authorized users.

✉ S. Karuthapandian
drpandianskvhnsnc2007@gmail.com

[1] Department of Chemistry, V. H. N. Senthikumara Nadar College (Autonomous), Virudhunagar, Tamil Nadu, India

[2] Department of Physics, V. H. N. Senthikumara Nadar College (Autonomous), Virudhunagar, Tamil Nadu, India

characteristics. For instance, multiple valence cations that includes Ce^{3+}, Yb^{3+}, Er^{3+} has been studied by Feng [13] and his research group for colloidal SCs. Rudra et al. [14] fabricated nitrogen doped ceria decorated aminated graphene for high performance SC electrodes. Majumder [15] and his research team synthesized rare-earth metal oxide incorporated polyindole nanocomposite for energy storage applications. Especially, gadolinia (Gd_2O_3), a versatile rare-earth material/Faradic electrode material because of its most accessible layered structure, redox activity, good electrochemical properties, high temperature resistant, high photocatalytic activity/stability, and self-regeneration [16–18]. Moreover, gadolinia can exist in two forms (monoclinic and base centred cubic structure) having different inter planner spacing which highly favours electrochemical process. Xu et al. [19] studied the gadolinium doped ternary composite for enhanced energy storage. Manavalan and his research group [20] fabricated gadolinia decorated reduced graphene oxide nanocomposite for sensing applications. Electrosynthesis of worm-like gadolinia and its nanocomposite were synthesized by Shiri and Ehsani [21]. Moreover, the gadolinia/polymer nanocomposite prepared by the same group could capable of deliver a specific capacitance of 300 F g^{-1}. Yet, the energy density of gadolinia based SC is still far behind that of rechargeable batteries (10^1–10^2 W h kg^{-1}). Such drawbacks in Gd based electrodes could be overcome by two strategies, (i) hybridization of carbonaceous material and (ii) tailoring of other electrode material the transition metal sulphide (TMS). In the first approach, a carbon rich electrode offer excellent cycle life and power density but fails to provide high capacity/energy density. Therefore, tailoring gadolinia with an electroactive species (TMS) is expected to solve the aforementioned issue. Probably, it will enhance the conductivity of the parent matrix and thereby considerably leading to a SC with volumetric energy density and excellent cycle life. Also, it may increases the mechanical strength of the tailored electrode material.

Among the metal sulphide family, nickel sulphide (NiS_x), a Faradic battery type electrode material, has salient electrochemical features like good redox activity (alkaline medium), high theoretical capacitance, excellent cycle life and high electronic conductivity [22–24]. Nandhini et al. [25] fabricated Ni_3S_4 nanoflakes via facile hydrothermal approach and it provides a maximum specific capacitance of 1184 F g^{-1} at a constant current density of 5 A g^{-1}. Parveen and his team [26] designed a symmetric SC utilizing NiS electrodes and the fabricated device could able to deliver a specific capacitance of 11 F g^{-1} with the energy density of 0.329 W h kg^{-1}. Hung et al. [27] studied the charge storage mechanism of NiS based electrodes prepared by laser irradiation method. Such intriguing positive aspects in NiS_x inspiring us to enhance the electrochemical performance of the gadolinia based electrodes. For the first time, we have devised to fabricate the novel electrode (gadolinia and nickel sulphide based electrode) for energy storage applications with fantastic recyclability.

Synthesis of rare-earth-based metal oxides still remains a tough task to build a desirable nanostructure with physicochemical properties and effective surface area. Various nanostructures of (Gd_2O_3) that includes nanoflakes, nanorods, nanodiscs and nanoflowers [28–31] have been fabricated using different synthetic methods. In the present investigation, porous gadolinia microspheres were designed by simple chemistry approach followed by the two step hydrothermal approach and explored its potential in SC domain.

2 Experimental section

2.1 Chemicals

Analytical grade of gadolinium(III) acetate hydrate (99.9%, Sigma Aldrich), sodium hydroxide pellets (99%, Sigma Aldrich), nickel nitrate (99.9%, Sigma Aldrich) and sodium thio sulphate (99.9%, Sigma Aldrich) were purchased and used as such.

2.2 Synthesis of gadolinium oxide/nickel sulphide microspheres

Detailed info about the preparation of gadolinium oxide and nickel sulphide nanostructure was prepared in the present study and the detailed synthetic protocol is provided in the Supporting Information. Gadolinium oxide/nickel sulphide microspheres have been prepared by simple solution mixing technique. In the typical synthesis, 0.5 g of gadolinium oxide and 0.5 g of nickel sulphide was dispersed in 50 mL of double distilled water separately and kept in sonicater for 15 min in room temperature. After that, the gadolinium oxide solution was stirred for 30 min and the nickel sulphide solution was transferred into the gadolinium solution (5 mL min^{-1}). Later, it was subjected to constant stirring at 300 rpm for 3 h. Finally, the product was collected by centrifugation. The collected product has been dried at 80 °C to yield gadolinium oxide/nickel sulphide nanoarchitecture. The synthesized material is named as GNMS (gadolinium oxide/nickel sulphide micro spheres) in further discussions.

2.3 Characterization techniques

The XRD patterns of the prepared materials were recorded using Philips PW-1710 X-ray diffractometer with Cu Kα radiation source (wavelength = 1.5406 Å), within the 2θ range of 10° to 80° at a step size of 0.05°. An IR Affinity-1S Fourier transform infrared spectrometer (Shimadzu, Japan) was used to record FTIR spectrum. Nitrogen adsorption/

desorption isotherms, pore size distribution and surface area of the prepared sample was examined by N_2 adsorption at 77 K on a Quantachrome® ASiQwin analyzer. The pore size distribution was estimated using Barrett–Joyner–Halenda (BJH) method. The morphological features of the fabricated composite was analysed using field emission scanning electron microscope (FE-SEM), SUPRA-40 at an accelerating voltage of 30 kV and high resolution transmission electron microscope (HR-TEM) JEOL/JEM 2100 having LaB_6-source at an operating voltage of 200 kV.

2.4 Fabrication of electrodes

The electrochemical behaviour of GNMS was examined in 2 M KOH solution using three/two electrode terminal in an electrochemical workstation (CH Instruments, USA). The three electrode configuration consists of the working electrode, counter electrode (Pt wire) and the reference electrode (Ag/AgCl). The working electrode has been prepared as follows: initially, 0.5 mg of active material (consists of 85% of GNMS, 10% of activated carbon and 5% of poly tetrafluoroethylene) was dispersed in 50 µL of ethanol and allowed to ultrasonicate for 5 min. Then, the slurry like material has been coated on the pretreated Ni foam (5% HCl/acetone/distilled water) in the area of 1 * 1 cm^2. Finally, it was dried at 80 °C to yield the working electrode. The supercapacitive features associated with GNMS electrodes were probed by cyclic voltammetry, galvanostatic charge discharge method and ac-impedance measurements.

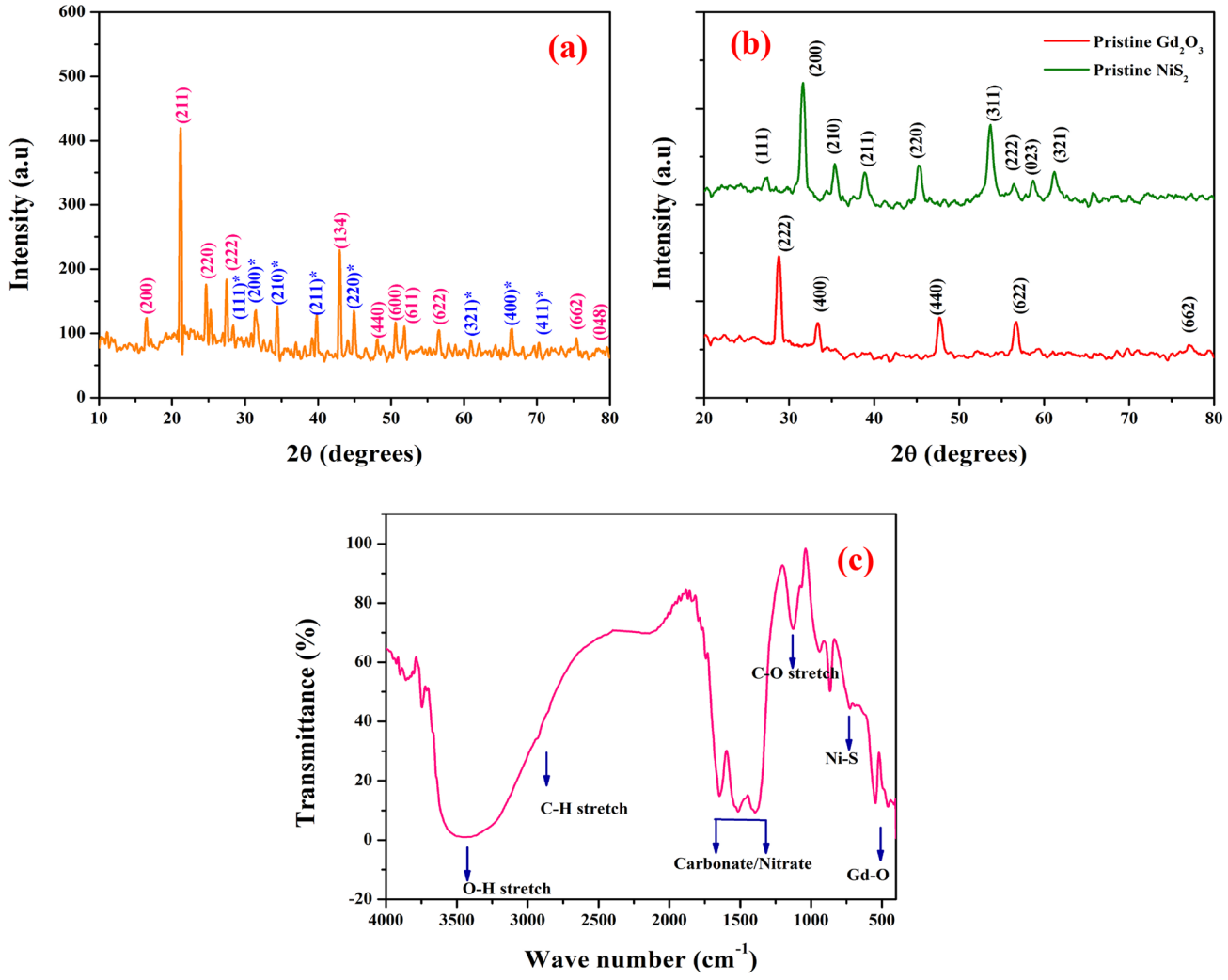

Fig. 1 **a** XRD pattern of gadolinium oxide/nickel sulphide nanostructures, **b** XRD patterns of pristine Gd_2O_3 and NiS_2 and **c** FTIR spectrum of GNMS sample

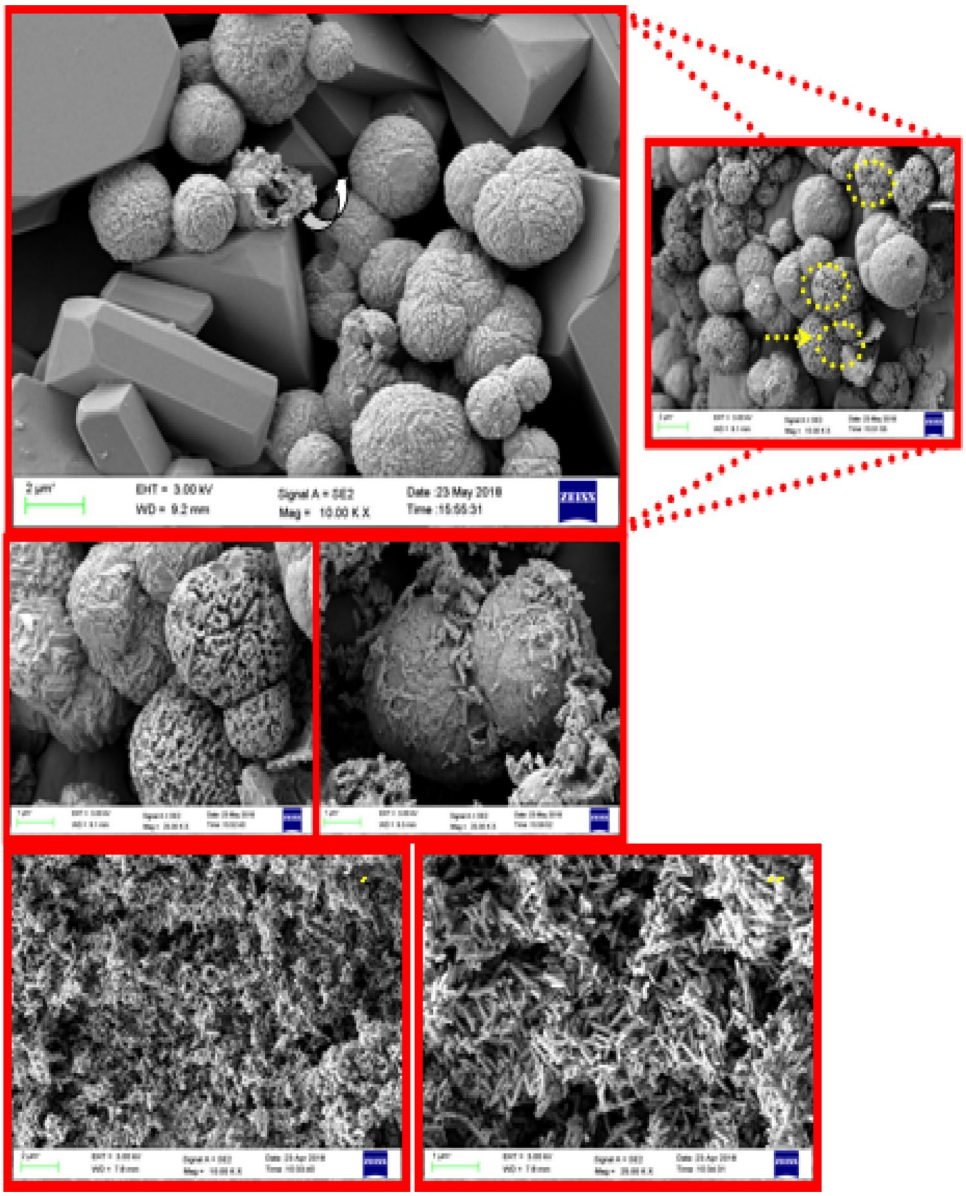

Fig. 2 **a**–**d** FE-SEM images of GNMS sample recorded at different magnifications and **e**, **f** FE-SEM images of pristine gadolinium oxide

3 Results and discussions

3.1 Structural, textural and morphological investigations

Figure 1a shows the XRD spectrum of GNMS, indicating the high degree crystallinity of the prepared materials. The diffraction peaks located at 2θ the position 16.38°, 20.10°, 23.25°, 28.58°, 42.6°, 47.54°, 50.62°, 52.11°, 56.42°, 76.81°, and 79.19° corresponding to (200), (211) (220), (222), (134), (440), (600), (611), (622), (662) and (048) planes of cubic phase Gd_2O_3 (JCPDS File No. 86–2477) with the space group of *la*3. The XRD patterns of pristine Gd_2O_3 and NiS_2 are provided in Fig. 1b. Moreover, the additional peaks present in the spectrum were indexed to the cubic structured NiS_2 and well agrees with the JCPDS File No. 89–3058.

The FTIR spectrum of gadolinium oxide/nickel sulphide nanocomposite was presented in Fig. 1c, which indicates the characteristic IR bands, corresponds to the Gd_2O_3 and NiS_2. The band centred at 555 cm^{-1} is attributable to Gd–O stretching mode [32] while 733 cm^{-1} corresponds to the characteristic Ni–S [33]. The bands located at the wave numbers 1120 cm^{-1} and 3454 cm^{-1} are assigned to the C–H stretching mode and O–H stretching mode of water molecules [34]. Further, the band around 1344–1662 cm^{-1} agreed with nitrate ions, which is present in the precursors [35].

FE-SEM and HR-TEM analysis has been employed to identify the morphological features of the prepared nanocomposite. Figure 2a–d shows the representative FE-SEM

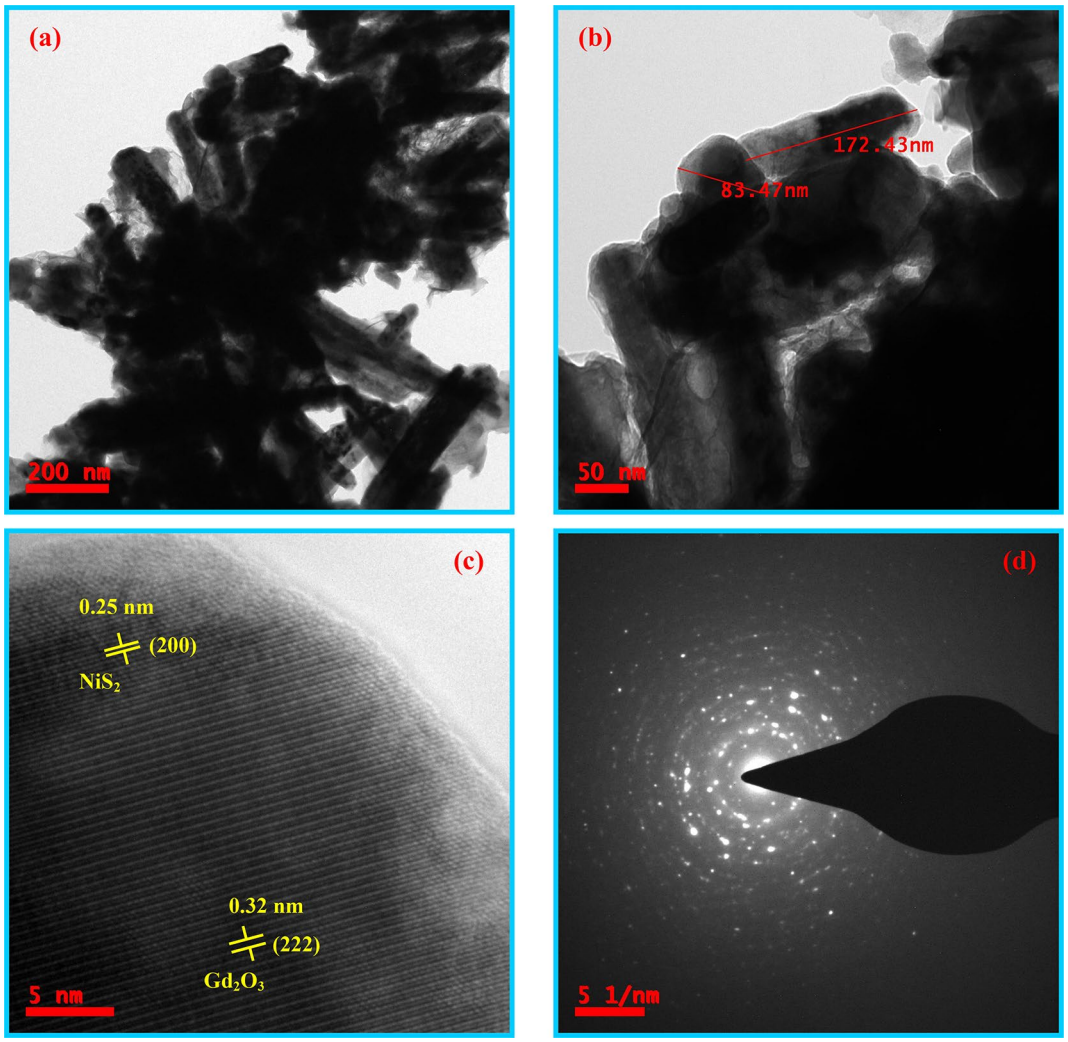

Fig. 3 **a**–**c** HR-TEM images of GNN sample recorded at different magnifications and **d** corresponding SAED pattern

images of gadolinium oxide–nickel sulphide nanocomposite. FE-SEM images of pristine gadolinium oxide (Fig. 2e, f) reveal the formation of two dimensional thick sheets. As we have already demonstrated in schematic representation, sheet like gadolinium ions encapsulates the nickel sulphide and results in porous microspheres. Of course, the presence brick like morphology is absolutely none other than gadolinium architecture. During the nucleation stage, the gadolinium ions that are not involved in the Vander Waals interaction [36, 37] gets aggregated and grows into brick like morphology. The FE-SEM images also reveal that spherical morphology composed of porous interconnected wrinkled nanosheets. In clear vision, plenty of pores could be seen in all the microspheres. As well-known, the pores can provide a larger pool for the access of electrolyte and helps ion transport, thereby favouring capacitance enhancement. Obviously, the hollow interior can be easily evidenced from some cracked spheres which facilitate mobilization of ions.

Further, to understand the basic building blocks of the prepared composite, HR-TEM analysis has been used. Figure 3a–c shows the HR-TEM images of gadolinium oxide–nickel sulphide nanocomposite. HR-TEM images confirm that nanosheets are the bricks to develop this facile architecture. Interconnected sheet like morphology has been observed for the prepared nanocomposite. Such interconnected nanostructures provide surplus pathways for ion intercalation and favours high electrochemical activity [38]. Moreover, the crystal lattice inter planner distance has been estimated using the high magnification HR-TEM image (Fig. 3c). An inter planner distance of 0.25 nm and 0.32 nm correspond to the crystal planes of nickel sulphide (200) and gadolinium oxide (222).

The chemical composition and the presence of elements in the prepared architecture have been identified using EDS spectroscopy. Figure 4a depicts the EDS of Gd_2O_3–NiS_2 nanocomposite and the weight percentage of elements

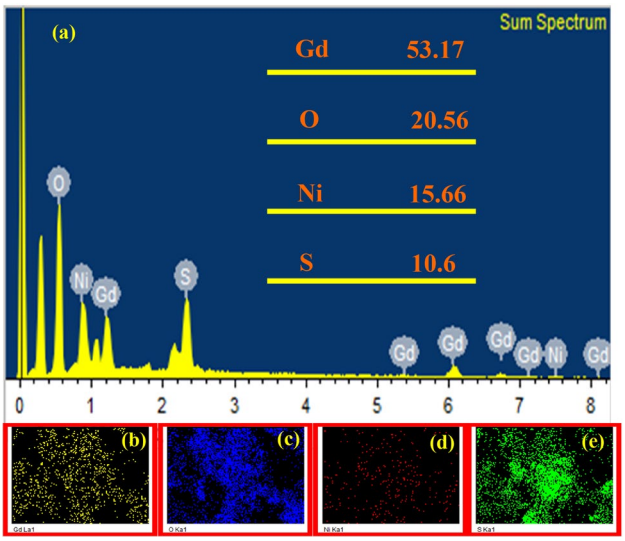

Fig. 4 **a** EDS of GNMS sample (inset wt% of elements), **b–e** elemental mapping of the prepared composite magnifications and **d** corresponding SAED pattern

present in the composite was presented in the inset. Added to that, the uniform distribution of all the elements in the GNMS has been confirmed through elemental mapping. Figure 4b–e presents the elemental mapping of the GNMS sample.

As evidenced from the morphological studies, presence of micro/meso pores in the prepared nanocomposite was further been analysed using BET measurements and their results are shown in Fig. 5a–c. The N_2 isotherm shows a sharp capillary condensation at high relative pressure (0.8–1) and it could be correspond to the type IV Langmuir isotherms [39]. This confirms the presence of high degree of pores (mesopores) in the prepared composite. Further, the pore size distribution was estimated from desorption isotherms using BJH model.

The pores are centred at 1.58 nm, 2.41 nm, 3.31 nm, 5.49 nm and 19.4 nm, respectively. Due to the creation of more mesopores, the prepared material can possess high specific area (11.82 $m^2\ g^{-1}$) with excellent pore volume (0.045 $cm^3\ g^{-1}$) that favours the accumulation of more charges on the electrode/electrolyte interface and considerably improves SC performance. Further, to estimate the surface area of the micropores De-Bore's *t*-plot was used. Figure 5c shows the *t*-plot of GNMS sample, indicating two linear segments which get deviated around 0.6 nm reveals the complete formation of micropores. From the *t*-plot, the surface area of the micropores has been estimated and it was found to be 9.789 $m^2\ g^{-1}$. Presence of high degree mesopores creates a plenty of voids thereby enhancing the specific surface area of the sample and results in excellent electrochemical performance [40].

3.2 Electrochemical Performance of GNMS

The electrochemical properties associated with GNMS electrodes were studied in order to explore their potential in SC domain. In the conventional three electrode set up (electrodes briefly discussed in Sect. 2.4), all the electrochemical characterizations were executed in 2 M KOH (electrolyte). The cyclic voltammetric responses have been recorded in the potential range of 1 V (from − 0.5 to 0.5 V). Figure 6a shows the cyclic voltammograms of gadolinium oxide/nickel sulphide nanocomposite which indicates a pair of redox peaks (+ 0.16 V, − 0.67 V) suggesting the charge storage mechanism was accomplished by fast Faradic redox phenomenon. Interestingly, the shift in peaks has been monitored in the CV profile and this is due to the incomplete neutralization of electrolyte ions and internal resistance developed in the electrode material [41]. Further, the specific capacitance of the electrode material has been estimated using the relation [37]

$$C_S = \frac{\int I dV}{2mv}, \tag{1}$$

where $\int I dV$ represents area enclosed by the CV curve (A V), m is the mass of the electroactive material (mg), ΔV is the potential window (V), ν is the scan rate (mV s^{-1}). A maximum specific capacitance of 232 F g^{-1} has been obtained for GNMS electrodes at a scan rate of 3 mV s^{-1}. The electrochemical impact of brick shaped particles, i.e. pristine Gd_2O_3 has been studied and reported in Supporting Information (S1). As noticed that, the specific capacitance of the electrode material decreases with increase in scan rate (Fig. 6b). The reason behind the fact that the electrode/electrolyte ions utilizes the interior/exterior surface of the electrode material at lower scan rates whereas at higher scans, ions have inadequate time to utilize both the surfaces (only at exterior parts) [42].

Further, the rate performance, charge capability and durability of the prepared electrodes were also investigated by galvanostatic charge/discharge method. The charge–discharge characteristics was performed for different current densities (0.5–10 A g^{-1}) in a potential range of 1 V (− 0.5 V to 0.5). Figure 6c depicts the GCD plateaus of gadolinium oxide/nickel sulphide nanocomposite recorded at various current densities, portrays that the capacitance of electrode material was mainly governed by redox process (non-linear plot).

Further, the specific capacitance of the electrode material has been estimated from the discharge area of the GCD profile using the relation [37]

$$C_S = \frac{2I \int V dt}{m\Delta V}, \tag{2}$$

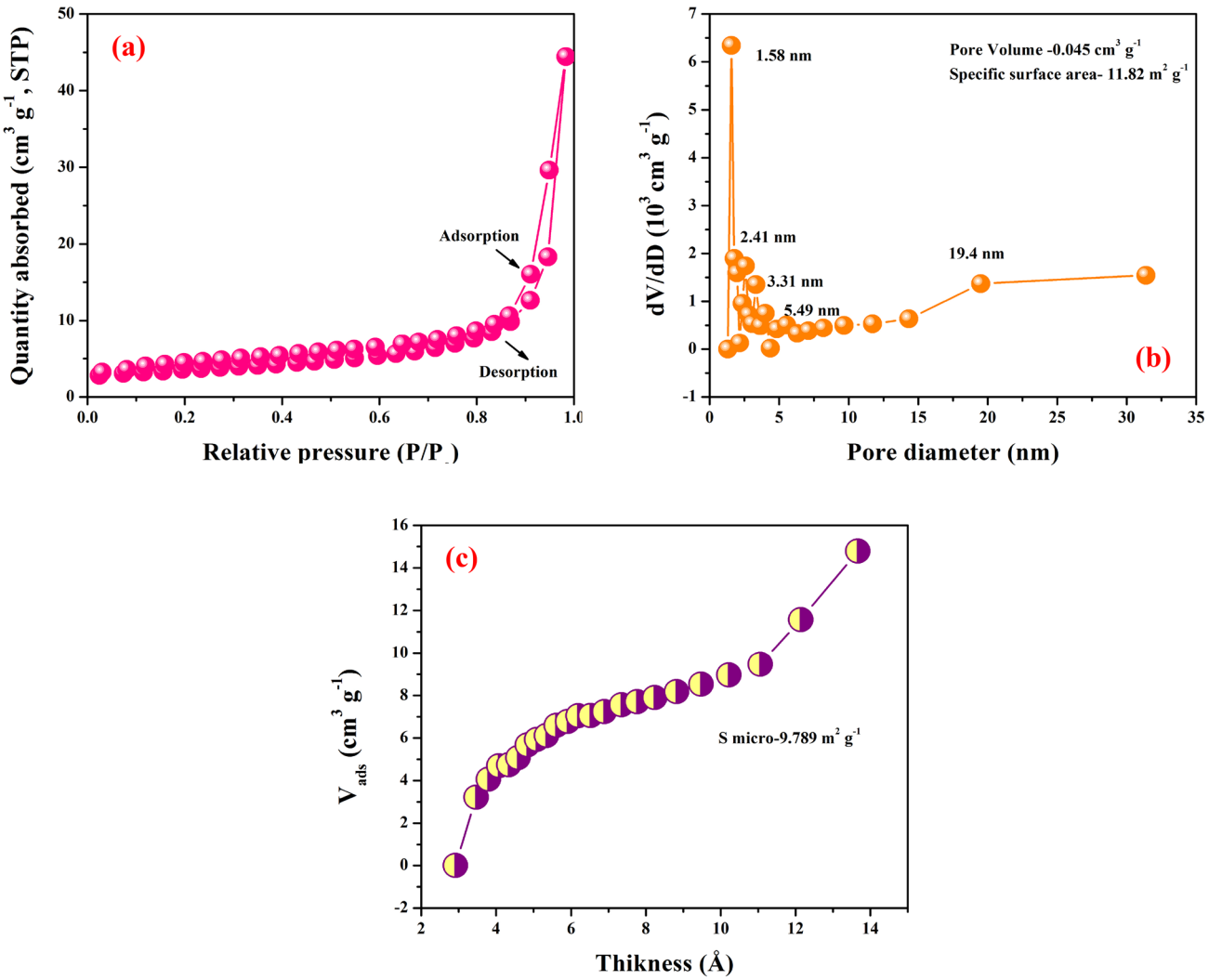

Fig. 5 **a** Nitrogen adsorption/desorption isotherms of GNMS, **b** pore size distribution profile and **c** corresponding *t*-plot

where I is the specific discharge current, (mA), m is the active mass of the electrode material (mg), ΔV is the potential window (V) and $\int V\mathrm{d}t$ is the area under the discharge curve (V s). From the GCD measurements, the calculated specific capacitance was found to be 354 F g^{-1} at a current density of 0.5 A g^{-1}.

This excellent capacitive behaviour is attributed to the presence of porous sheet like architecture which provides uninterrupted pathways for the mobilization of electrolyte ions. It noteworthy to mention that, the capacitance of the electrode materials decreases when the current density increases (Fig. 6d). It is due to two major reasons, (i) IR drop at high current densities and (ii) internal resistance of the electrode material [43]. The Coulombic efficiency at low current (1 A g^{-1}) is quite higher than the high current which is attributed to the irreversibility of Nernstian phenomenon [35, 39]. At lower current, ions have enough time to intercalate and favours in admirable efficiency. But, the migration and intercalation of electrolyte ions have been restricted due to the inadequacy of time at low current densities and results in low electrochemical performance.

The capacitive, resistive and ionic conductivity of the GNMS electrodes has been checked using electrochemical impedance spectroscopy. Figure 7a shows the impedance spectrum of GNMS sample recorded at a bias potential of 90 mV within the frequency range of 0.01 to 100 Hz. The obtained impedance data were fitted to the equivalent Randle circuit and it was provided in the Fig. 7a (inset). The impedance spectrum consists of two portions, (i) high frequency region (semi-circle region) which is corresponds to the charge transfer resistance developed due to the Faradic

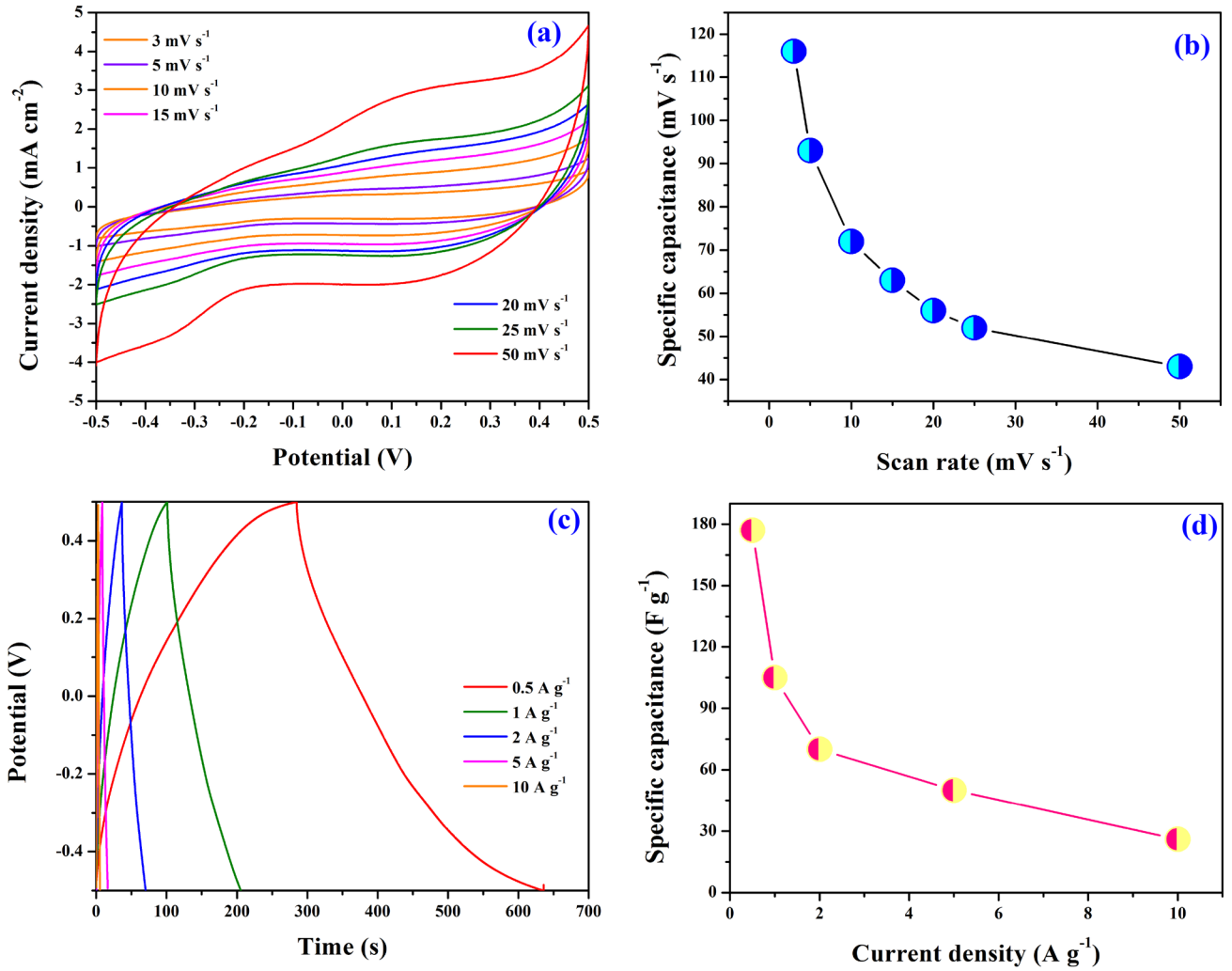

Fig. 6 **a** CV profile of GNN electrodes recorded at various scan rates (Ag vs AgCl), **b** effect of scan rate against specific capacitance, **c** GCD plot of gadolinium oxide/nickel sulphide nanocomposite at different current densities and **d** variation of specific capacitance with current densities

redox process. (ii) Low frequency region (linear segment) corresponds to the Warburg resistance.

The estimated charge transfer resistance and equivalent series resistance for the prepared nanocomposite were found to be 6.37 Ω and 2.7 Ω. A charge transfer resistance of 6.23 Ohm was estimated from the electrochemical impedance spectrum with the help of modified Randle's circuit. This implies that low charge transfer resistance probably enhances the electrochemical performance [42] of the prepared nanocomposite. This low R_{ct} value enhances the conductivity of the electrode material and significantly improves the electrochemical performance [44]. Figure 7b, illustrates the variation of specific capacitance against frequency. The gadolinium oxide/nickel sulphide nanostructure exhibits a specific capacitance of 77 F g^{-1} at a frequency of 0.01 Hz.

Further, the practical utility of the electrodes has been checked by executing the stability test for the prepared electrode materials. The cyclic life of the electrodes were checked by 5000 continuous charge/discharge cycles at a current density of 5 A g^{-1} (Fig. 8). For the first 2000 cycles, slight up and down variation in specific capacitance has been monitored (electrode material gets activated). After that, the specific capacitance increases gradually for the next 2000 cycles. At the end of 5000 cycles, 1.3% loss in specific capacitance has been observed.

Furthermore, the Coulombic efficiency of the electrodes were also diagnosed from the 5000 cycles using the relation [35],

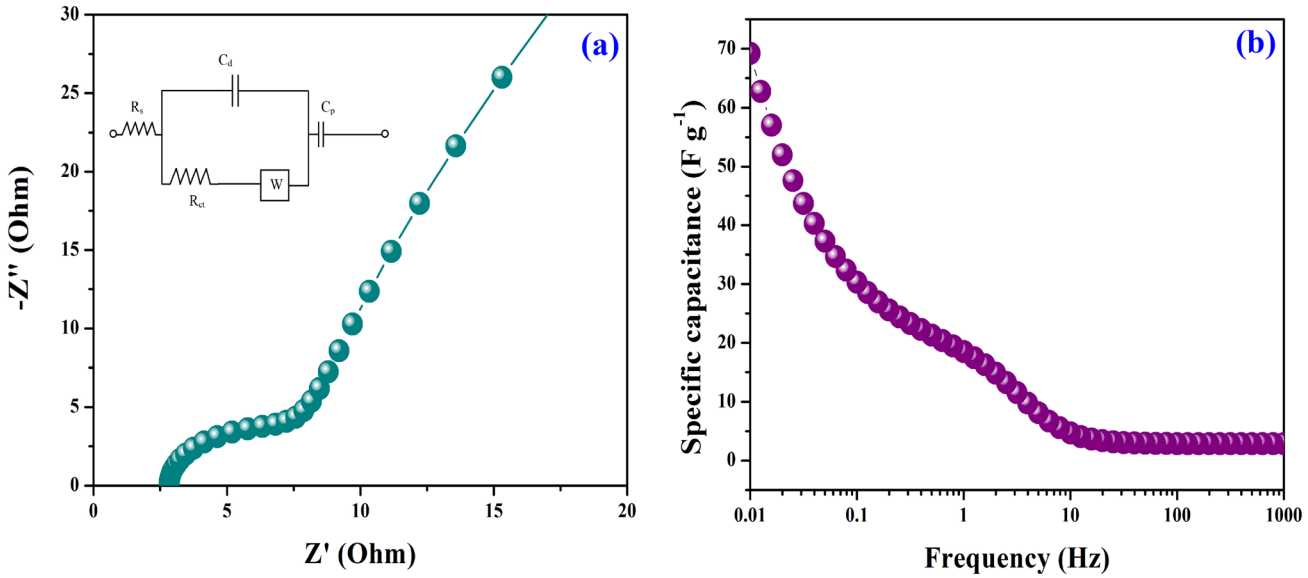

Fig. 7 **a** Impedance spectrum of GNN electrode recorded at a bias potential of 90 mV, inset modified Randle's circuit and **b** frequency dependence of specific capacitance

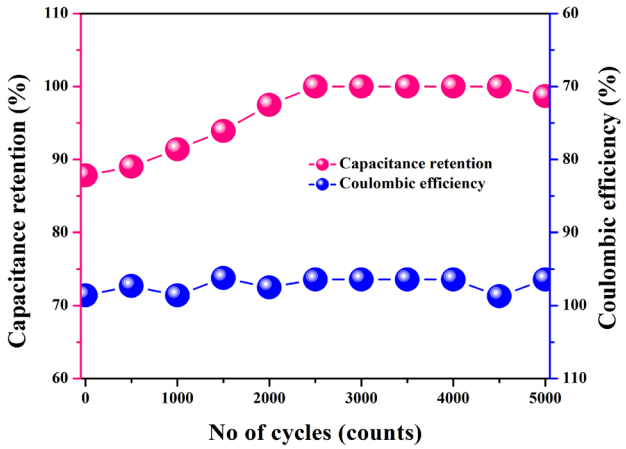

Fig. 8 Cyclic life and Coulombic efficiency profile of GNMS electrodes recorded for 5000 cycles at a current density of 5 A g^{-1}

$$\eta = \frac{t_d}{t_c}, \tag{3}$$

where η the Coulombic efficiency, t_d is the discharge time and t_c is the charging time. After the end of 5000 continuous charge discharge cycles, the electrode material exhibits 96.4% efficiency.

4 Conclusions

In conclusion, we have fabricated gadolinia based electrodes for energy storage applications with enhanced electrochemical performance by tailoring with high conductivity nickel sulphide. Analytical investigation reports reveal that the fabricated composite is composed of mesoporous interconnected nanosheets which facilitate uninterrupted pathways for ion transport. Moreover, an ultra-high specific surface area provides a numerous vacancies for ions which are involved in the electrochemical phenomenon and it results in excellent supercapacitive nature. Furthermore, the fabricated electrode exhibits a negligible amount of degradation in capacitance after long-term durability. The present study opens up a new pathway in developing new Faradic earth metal oxide/metal sulphide composite materials for future energy systems.

References

1. H. Banda, S. Perie, B. Daffos, P.L. Taberna, L. Dubois, O. Crosnier, P. Simon, D. Lee, G.D. Paepe, F. Duclairoir, Sparsely pillared graphene materials for high performance supercapacitors: improving ion transport and storage capacity. ACS Nano **13**, 1443 (2019)
2. Y. Lin, Z. Chen, C. Yu, W. Zhong, Heteroatom-doped sheet like and hierarchical porous carbon based on natural biomass small molecule peach gum for high-performance supercapacitors. ACS Sustain. Chem. Eng. **7**, 3389 (2019)
3. B. Liu, Y. Liu, H. Chen, M. Yang, L. Huaming, MnO_2 nanostructures deposited on graphene-like porous carbon nanosheets for high-rate performance and high-energy density asymmetric supercapacitors. ACS Sustain. Chem. Eng. **7**, 3101 (2019)

4. S. Schweizer, J. Landwehr, B.J.M. Etzold, R.H. Meibner, M. Amkreutz, P. Schiffels, J.R. Hill, Combined computational and experimental study on the influence of surface chemistry of carbon-based electrodes on electrode–electrolyte interactions in supercapacitors. J. Phys. Chem. C **123**, 2716 (2019)
5. Z. Yu, L. Tetard, L. Zhai, J. Thomas, Supercapacitor electrode materials: nanostructures from 0 to 3 dimensions. Energy Environ. Sci. **8**, 702 (2015)
6. D. Bresser, D. Buchhoiz, A. Moretti, A. Varzi, S. Passerini, Alternative binders for sustainable electrochemical energy storage the transition to aqueous electrode processing and bio-derived polymers. Energy Environ. Sci. **11**, 3096 (2014)
7. K. Ramakrishnan, C. Nithiya, R. Karvembu, Heterostructure of two different 2D materials based on MoS_2 nanoflowers @ rGO: an electrode material for sodium-ion capacitors. Nanoscale Adv. **1**, 334 (2019)
8. H. Du, Y. Pan, X. Zhang, F. Cao, T. Wan, H. Du, R. Joshi, C. Dewei, Silver nanowire/nickel hydroxide nanosheet composite for a transparent electrode and all-solid-state supercapacitor. Nanoscale Adv. **1**, 140 (2019)
9. C. Masarapu, H.F. Zeng, K.H. Hung, B. Wei, Effect of temperature on the capacitance of carbon nanotube supercapacitors. ACS Nano **3**, 2199 (2009)
10. Y. Zhu, S. Muralti, M.D. Stoller, K.J. Ganesh, W. Cai, P.J. Ferrera, A. Pirkle, R.M. Wallace, K.A. Cychosz, M. Thommes, D. Su, E.A. Stach, R.S. Ruoff, Carbon-based supercapacitors produced by activation of graphene. Science **332**, 1537 (2011)
11. K. Liu, Z. Hu, R. Xue, J. Zhang, J. Zhu, Electrodeposition of high stable poly (3, 4-ethylenedioxythiophene) in ionic liquids and its potential applications in electrochemical capacitor. J. Power Sources **179**, 858 (2008)
12. G. Wang, L. Zhang, J. Zhang, A review of electrode materials for electrochemical supercapacitors. Chem. Soc. Rev. **41**, 797 (2012)
13. K.F. Chen, D. Xue, Rare earth and transitional metal colloidal supercapacitors. Sci. China Technol. Sci. **58**(11), 1768 (2015)
14. R. Kumar, A. Agrawal, R.K. Nagarale, A. Sharma, High performance supercapacitors from novel metal-doped ceria-decorated aminated graphene. J. Phys. Chem. B **120**(6), 3107 (2015)
15. M. Majumder, R.B. Choudhary, A.K. Thakur, C.S. Rout, G. Gupta, Rare earth metal oxide (RE_2O_3; RE = Nd, Gd, and Yb) incorporated polyindole composites: gravimetric and volumetric capacitive performance for supercapacitor applications. N. J. Chem. **42**(7), 5295 (2018)
16. E.W. Awin, S. Sridar, R. Shabadi, R. Kumar, Structural, functional and mechanical properties of spark plasma sintered gadolinia (Gd_2O_3). Ceram. Int. **42**, 1384 (2016)
17. J. Zhang, W. Wu, S. Yan, G. Chu, S. Zhao, Enhanced photocatalytic activity for the degradation of Rhodamine B by TiO_2 modified with Gd_2O_3 calcined at high temperature. Appl. Surf. Sci. **344**, 249 (2015)
18. H. Zho, L. Melro, T.D. Camargo, C. Isnaldi, D.D. Souza, F. Duarte, D. Ananias, E.B. Lami, A.M.D. Santos, A.B. Timmons, Adsorption study of a macro-RAFT agent onto SiO_2-coated Gd_2O_3:Eu^{3+} nanorods: requirements and limitations. Appl. Surf. Sci. **394**, 519 (2017)
19. G.B. Xu, L.W. Yang, X.L. Wei, J.W. Ding, J.X. Zhong, P.K. Chu, Highly-crystalline ultrathin gadolinium doped and carbon-coated $Li_4Ti_5O_{12}$ nanosheets for enhanced lithium storage. J. Power Sources **295**, 305 (2015)
20. S. Manavalan, U. Rajai, S.M. Chen, T.W. Chen, R.J. Ramalingam, T. Maiyalagan, A. Sathiyan, Q. Hao, W. Lei, Microwave-assisted synthesis of gadolinium(III) oxide decorated reduced graphene oxide nanocomposite for detection of hydrogen peroxide in biological and clinical samples. J. Electroanal. Chem. **837**, 167 (2019)
21. H.M. Shiri, A. Ehsani, Pulse electrosynthesis of novel worm-like gadolinium oxide nanostructure and its nanocomposite with conjugated electroactive polymer as a hybrid and high efficient electrode material for energy storage device. J. Colloid Interface Sci. **484**, 70 (2016)
22. Y. Zhang, F. Lu, L. Pan, Y. Xu, Y. Yang, Y. Bando, D. Golberg, J. Yao, X. Wang, Improved cycling stability of NiS_2 cathode through designing "Kiwano" hollow structure. J. Mater. Chem. A **6**, 11978 (2013)
23. X.Y. Yu, X.W. Lou, Mixed metal sulphides for electrochemical energy storage and conversion. Adv. Energy Mater. **8**(3), 1701592 (2017)
24. Y. Zhang, W. Sun, X. Rui, B. Li, L.H. Tan, G. Guo, S. Madhavi, Y. Zong, Q. Yan, One-pot synthesis of tunable crystalline Ni_3S_4 @ amorphous MoS_2 core/shell nanospheres for high-performance supercapacitors. Small **11**(30), 201403772 (2015)
25. N.S. Muthu, M. Gopalan, Mesoporous nickel sulphide nanostructures for enhanced supercapacitor performance. Appl. Surf. Sci. **480**, 186 (2019)
26. N. Praveen, S.A. Ansari, S.G. Ansari, H. Fouad, M. Nasser, M.A. Salam, M.H. Cho, Solid-state symmetrical supercapacitor based on hierarchical flower-like nickel sulphide with shape-controlled morphological evolution. Electrochim. Acta **268**, 82 (2018)
27. T.Z. Hung, Z.W. Yin, S.B. Betzler, W. Zheng, J. Yang, H. Zheng, Nickel sulphide nanostructures prepared by laser irradiation for efficient electro-catalytic hydrogen evolution reaction and supercapacitors. Chem. Eng. J. **367**, 115 (2019)
28. F. Abed, M. Aghazadeh, B. Arhami, Preparation of Gd_2O_3 coral-like nanostructure by pulse electrodeposition-heat-treatment method. Mater. Lett. **99**, 11 (2013)
29. M.W. Ahmad, C.R. Kim, J.S. Baeck, Y. Chang, T.J. Kim, J.E. Bae, K.S. Chae, G.H. Lee, Bovine serum albumin (BSA) and cleaved-BSA conjugated ultrasmall Gd_2O_3 nanoparticles: synthesis, characterization, and application to MRI contrast agents. Colloids Surf. A **450**, 67 (2014)
30. N. Babayevska, G. Nowaczyk, M. Jarek, K. Zaleski, S. Jurga, Synthesis and study of bifunctional core–shell nanostructures based on ZnO @ Gd_2O_3. J. Alloys Compds **672**, 350 (2016)
31. I.A. Mkhalid, Photocatalytic remediation of atrazine under visible light radiation using Pd–Gd_2O_3 nanospheres. J. Alloys Compds **682**, 766 (2016)
32. T. Grzyb, R.J. Wiglusz, V. Nagimyi, A. Kotlov, S. Lis, Revised crystal structure and luminescent properties of gadolinium oxyfluoride $Gd_4O_3F_6$ doped with Eu^{3+} ions. Dalton Trans. **43**, 6925 (2014)
33. S. Pan, J. Zhu, X. Liu, Preparation, electrochemical properties, and adsorption kinetics of Ni_3S_2/graphene nanocomposites using alkyldithiocarbonatio complexes of nickel(II) as single-source precursors. N. J. Chem. **37**, 654 (2013)
34. S. Vadivel, D. Maruthamani, M. Kumaravel, B. Saravanakumar, B. Paul, S.D. Siddhartha, S. Dhar, K. Saravanakumar, V. Muthuraj, Supercapacitor studies on $BiPO_4$ nanoparticles synthesized through a simple microwave approach. J. Taibah Univ. Sci. **11**, 661 (2017)
35. J.J. William, I.M. Babu, G. Muralidharan, Microwave-assisted fabrication of L-arginine capped α-$Ni(OH)_2$ @ microstructures as an electrode material for high performance hybrid supercapacitors. Mater. Chem. Phys. **224**, 357 (2019)
36. S. Vijayakumar, S. Nagamuthu, G. Muralidharan, Porous NiO/C nanocomposites as electrode material for electrochemical supercapacitors. ACS Sustain. Chem. Eng. **1**(9), 1110 (2013)
37. I.M. Babu, J.J. William, G. Muralidharan, Carboxymethyl cellulose aided fabrication of flaky structured mesoporous β-$Co(OH)_2$/C nanocomposite for supercapacitors. J. Mater. Sci. Mater. Electron. **30**(3), 2107 (2019)

38. B. Saravanakumar, K.K. Purushothaman, G. Muralidharan, Interconnected V_2O_5 nanoporous network for high-performance supercapacitors. ACS Appl. Mater. Interfaces **4**, 4484 (2012)
39. I.M. Babu, J.J. William, G. Muralidharan, Ordered mesoporous Co_3O_4/CMC nanoflakes for superior cyclic life and ultra high energy density supercapacitor. Appl. Surf. Sci. **480**, 371 (2019)
40. J.J. William, I.M. Babu, G. Muralidharan, Spongy structured α-$Ni(OH)_2$: facile and rapid synthesis for supercapattery applications. Mater. Lett. **238**, 35 (2019)
41. I.M. Babu, J.J. William, G. Muralidharan, Surfactant tuned morphology of mesoporous β-$Co(OH)_2$/CMC nanoflakes: a prospective candidate for supercapacitors. J. Solid State Electrochem. **23**, 1325 (2019)
42. K.K. Purushothaman, B. Saravanakumar, I.M. Babu, B. Sethuraman, G. Muralidharan, Nanostructured CuO/reduced graphene oxide composite for hybrid supercapacitors. RSC Adv. **4**, 23485 (2014)
43. I.M. Babu, K.K. Purushothaman, G. Muralidharan, Ag_3O_4 grafted NiO nanosheet for high performance supercapacitors. J. Mater. Chem. A **3**, 420 (2014)
44. I.M. Babu, J.J. William, G. Muralidharan, Hierarchical β-$Co(OH)_2$/CoO nanosheets: an additive free approach for supercapattery applications. Ionics **25**, 2437 (2019)